

## Dichotomy between Nodal and Antinodal Quasiparticles in Underdoped $(\text{La}_{2-x}\text{Sr}_x)\text{CuO}_4$ Superconductors

X. J. Zhou,<sup>1,2</sup> T. Yoshida,<sup>1,3</sup> D.-H. Lee,<sup>4,5</sup> W. L. Yang,<sup>2,1</sup> V. Brouet,<sup>1,2</sup> F. Zhou,<sup>6</sup> W. X. Ti,<sup>6</sup> J. W. Xiong,<sup>6</sup> Z. X. Zhao,<sup>6</sup> T. Sasagawa,<sup>1</sup> T. Kakeshita,<sup>7</sup> H. Eisaki,<sup>7</sup> S. Uchida,<sup>7</sup> A. Fujimori,<sup>3</sup> Z. Hussain,<sup>2</sup> and Z.-X. Shen<sup>1</sup>

<sup>1</sup>*Department of Physics, Applied Physics and Stanford Synchrotron Radiation Laboratory, Stanford University, Stanford, California 94305, USA*

<sup>2</sup>*Advanced Light Source, Lawrence Berkeley National Laboratory, Berkeley, California 94720, USA*

<sup>3</sup>*Department of Physics, University of Tokyo, Bunkyo, Tokyo 113, Japan*

<sup>4</sup>*Department of Physics, University of California at Berkeley, Berkeley, California 94720, USA*

<sup>5</sup>*Material Science Division, Lawrence Berkeley National Laboratory, Berkeley, California 94720, USA*

<sup>6</sup>*National Laboratory for Superconductivity, Institute of Physics, Chinese Academy of Sciences, Beijing 100080, China*

<sup>7</sup>*Department of Superconductivity, University of Tokyo, Bunkyo, Tokyo 113, Japan*

(Received 20 June 2003; published 6 May 2004)

High resolution angle-resolved photoemission measurements on an underdoped  $(\text{La}_{2-x}\text{Sr}_x)\text{CuO}_4$  system show that, at energies below 70 meV, the quasiparticle peak is well defined around the  $(\pi/2, \pi/2)$  nodal region and disappears rather abruptly when the momentum is changed from the nodal point to the  $(\pi, 0)$  antinodal point along the underlying “Fermi surface.” It indicates that there is an extra low energy scattering mechanism acting upon the antinodal quasiparticles. We propose that this mechanism is the scattering of quasiparticles across the nearly parallel segments of the Fermi surface near the antinodes.

DOI: 10.1103/PhysRevLett.92.187001

PACS numbers: 74.72.-h, 71.18.+y, 74.25.Jb

The high temperature superconductivity in cuprates is derived from doping the parent antiferromagnetic Mott insulators. It is found that the normal state properties of cuprates are highly anomalous, particularly in the underdoped region. Understanding the normal state is believed to be a key for understanding the mechanism of high temperature superconductivity [1]. For the underdoped cuprates, one peculiar behavior of its electronic structure, as revealed by angle-resolved photoemission spectroscopy, is the dichotomy between the  $\sim(\pi/2, \pi/2)$  nodal and  $\sim(\pi, 0)$  antinodal excitations. In underdoped  $\text{Bi}_2\text{Sr}_2\text{CaCu}_2\text{O}_8$  ( $\text{Bi}2212$ ), it was found that the line shape of the *normal state* photoemission spectra is broad in the antinodal region but sharp near the nodal region [2]. It was proposed that the antinodal spectral broadening in the normal state is due to the coupling of electrons with the  $(\pi, \pi)$  magnetic excitations [2].

The peculiar electronic structure of the underdoped sample may provide important clues for understanding the anomalous normal state properties. It is therefore essential to establish whether such a nodal-antinodal dichotomy is universal in cuprate materials and, particularly, to establish its physical origin. However,  $\text{Bi}2212$  is not an ideal system for such an in-depth investigation. Because of disorder, no sharp nodal structure has been observed in deeply underdoped  $\text{Bi}2212$ . Furthermore, the states near the antinodal region are severely complicated by its superstructure. This, together with the bilayer splitting resolved very recently [3], raises concerns about the interpretations [4–6]. The  $\text{La}_{2-x}\text{Sr}_x\text{CuO}_4$  (LSCO) system, in comparison, is an ideal candidate to address the issue in the underdoped region because the system

becomes less disordered with decreasing doping. Its simple crystal structure also makes it free from the complications of the superstructure and bilayer splitting encountered in  $\text{Bi}2212$ .

While the majority of photoemission work thus far has been performed on  $\text{Bi}2212$ , data on LSCO are available only recently because of the improved sample quality and better understanding of matrix element effects involved in measuring the LSCO system [7–9]. In this Letter, we present detailed angle-resolved photoemission data on underdoped LSCO superconductors. We observe a remarkably sharp nodal quasiparticle peak at all doping levels studied, even for heavily underdoped samples. In contrast, the antinodal peak exists only in optimally doped and overdoped samples. Particularly, these sharp peaks can be observed only at low energy, below 70 meV. In addition, for underdoped samples, when moving from nodal to antinodal regions, we find that the disappearance of sharp peaks occurs in a fairly abrupt fashion near where the Fermi surface changes from parallel to the  $(\pi, 0)$ - $(0, \pi)$  diagonal to parallel to the  $(0, 0)$ - $(\pi, 0)$  or  $(0, 0)$ - $(0, \pi)$  directions. Intrigued by the close tie between the quasiparticle scattering and the Fermi surface topology, we propose this “nodal-antinodal dichotomy” is due to the scattering of quasiparticles across the almost parallel segments of the Fermi surface near the antinodes.

The photoemission measurements were carried out on beam line 10.0.1 at Advanced Light Source (ALS), using a Scienta 2002 electron energy analyzer. The photon energy is 55 eV and the  $\vec{E}$  vector of the incident light is parallel to the  $\text{CuO}_2$  plane and  $45^\circ$  with respect to the Cu-O bond, as indicated by the arrow in Fig. 2(a) (below)

[7,8]. The energy resolution is 15–20 meV and the angular resolution is  $0.3^\circ$  ( $0.018 \text{ \AA}^{-1}$  in momentum). In this Letter, we mainly present our data on the underdoped LSCO ( $x = 0.063$ ,  $T_c = 12 \text{ K}$ ) and LSCO ( $x = 0.09$ ,  $T_c = 28 \text{ K}$ ) samples. For comparison, we also show data on overdoped LSCO ( $x = 0.22$ ,  $T_c = 24 \text{ K}$ ). The LSCO single crystals are grown by the traveling solvent floating zone method [10]. The samples were cleaved *in situ* in vacuum with a base pressure better than  $4 \times 10^{-11}$  Torr and measured at a temperature of  $\sim 20 \text{ K}$ .

Figure 1 presents experimental results along the  $(0, 0)$ - $(\pi, \pi)$  nodal direction of the LSCO ( $x = 0.063$ ) sample. Even for this extremely underdoped sample in the vicinity of an insulator-superconductor transition, one can see a remarkably sharp quasiparticle peak in the nodal region with a clear dispersion [Fig. 1(a)]. The sharp peak abruptly turns into an edge once it disperses up to an energy of  $\sim 70 \text{ meV}$ . Such a dramatic change in spectral shape is not observed in underdoped Bi2212 presumably due to its stronger disorder. The dispersion [Fig. 1(b)], extracted by fitting momentum distribution curves (MDCs) [9,11–14], shows a clear slope break (a kink) at an energy  $\sim 70 \text{ meV}$ . The MDC width, which is related to the scattering rate  $\tau^{-1}$ , also exhibits a drop at the same energy [inset of Fig. 1(b)]. All these observations indicate that there is an energy scale at  $\sim 70 \text{ meV}$  for the nodal quasiparticles.

Figure 2(a) shows the low energy spectral weight of the LSCO ( $x = 0.063$ ) sample as a function of momentum by

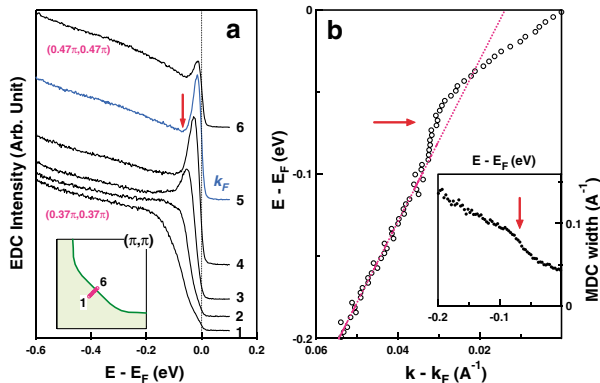


FIG. 1 (color). Electronic structure of LSCO ( $x = 0.063$ ,  $T_c = 12 \text{ K}$ ) along the  $(0, 0)$ - $(\pi, \pi)$  nodal direction [inset of Fig. 1(a)] at a temperature of 20 K. (a) EDCs measured along the nodal direction in a second Brillouin zone. The EDCs are numbered according to the momentum points in the inset. These momentum points are equal spaced: point 1 corresponds to  $(0.374\pi, 0.374\pi)$  and point 6 corresponds to  $(0.466\pi, 0.466\pi)$ . The red arrow indicates an energy of  $\sim 70 \text{ meV}$  below which the quasiparticle survives and above which it turns into a broad edge. (b) A kink in the dispersion at  $\sim 70 \text{ meV}$  as indicated by an arrow. The dotted pink line is a guide to the eye which is a line fitting the high-energy part of the dispersion. In the inset is the MDC width which shows a drop at an energy of  $\sim 70 \text{ meV}$ , as indicated by an arrow.

integrating energy distribution curves (EDCs) in a narrow energy window near  $E_F$  ( $-5 \text{ meV}$ ,  $5 \text{ meV}$ ) ( $k_x$  and  $k_y$  are along Cu-O bonding direction). The high intensity contour constitutes what we call the “Fermi surface.” To be quantitative, we used MDCs at  $E_F$  to extract the Fermi momentum ( $k_F$ ) by following the MDC peak position. This is exemplified in the inset of Fig. 2(a) for nine cuts in a second zone and the obtained  $k_F$  are marked as red crosses in Fig. 2(a). The  $k_F$  are obtained in another second zone and the first zone in a similar manner although the relative spectral intensity in the first Brillouin zone is much weaker. To a good approximation, the measured Fermi surface can be represented as three straight segments: two antinodal ones (marked black in Fig. 3) running parallel to  $(0, 0)$ - $(\pi, 0)$  and  $(0, 0)$ - $(0, \pi)$  directions, respectively, and the nodal one (marked red in Fig. 3) running parallel to the  $(\pi, 0)$ - $(0, \pi)$  diagonal direction.

Figures 2(b1), 2(b2), 2(b3), 2(b4), 2(b5), 2(b6), 2(b7), 2(b8), and 2(b9) show the EDCs along nine cuts of the Fermi surface from the nodal to the antinodal region [as marked in Fig. 2(a)] for the  $x = 0.063$  sample. The red curves are the EDCs at  $k = k_F$ . It is clear that all quasiparticle peaks are confined within the 70 meV energy range near the Fermi level. Moreover, the quasiparticle peaks exist only on part of the Fermi surface near the nodes, as marked by the solid red line in Fig. 3. Away from the “nodal segment” the peak gets weaker and disappears in a fairly abrupt fashion. This can be seen more clearly from Fig. 4(a) where the EDCs on the underlying Fermi surface and at  $(\pi, 0)$  are plotted together. A similar sharp transition is also observed in another underdoped LSCO ( $x = 0.09$ ) sample [Fig. 4(b)]. The situation for these underdoped samples is very different from that in the highly overdoped ( $x = 0.22$ ) sample [Fig. 4(c)]. In that case, we see a quasiparticle peak over the entire Fermi surface; the antinodal peak appears even sharper than the nodal peak. This doping dependence clearly indicates that the spectral broadening near the antinodal region in the underdoped samples is *not due to a matrix element effect*. This is also consistent with earlier observations in Bi2212 [2].

At first glance, the concept of quasiparticle seems entirely inappropriate for heavily underdoped cuprates. Given the fact that we are dealing with a strongly correlated system, the existence of sharp nodal quasiparticle below 70 meV is itself a miracle, not to mention the nodal-antinodal dichotomy. One might argue that the nodal-antinodal dichotomy is due to the much higher excitation energy near the antinodes compared to that near the nodes, as often assumed in the theory literature. We stress that the antinodal edge ( $\sim 15 \text{ meV}$ ) discussed in this Letter is not particularly high in energy compared to that of some nodal peaks (Fig. 4) and is definitely below 70 meV along the Fermi surface locus. Therefore, this trivial explanation does not work. The spirit of our Letter is to assume the existence of a mechanism that

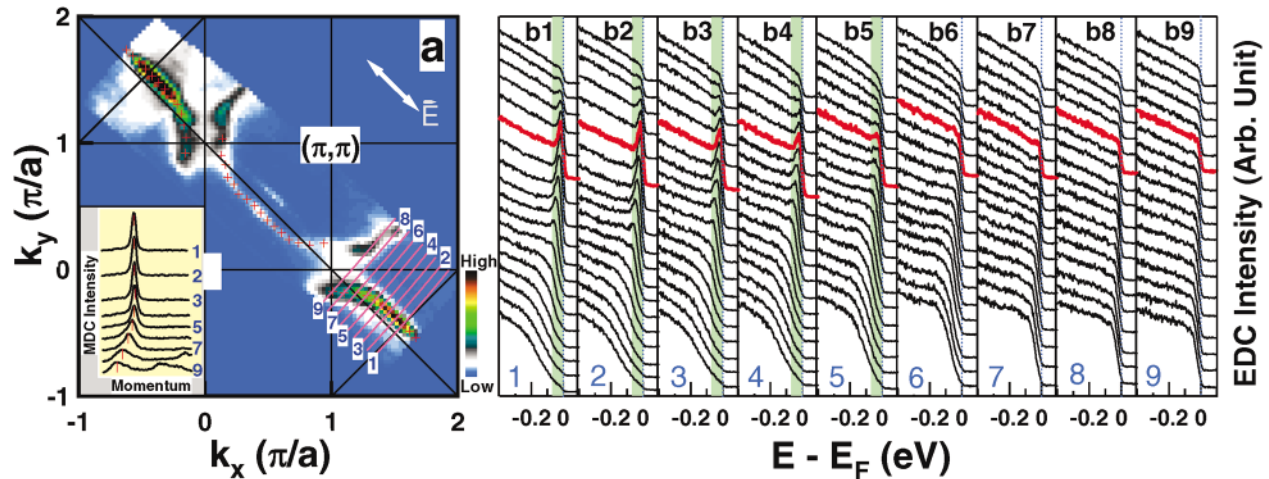


FIG. 2 (color). (a) Low energy spectral weight as a function of  $k_x$  and  $k_y$  for the LSCO  $x = 0.063$  sample measured at a temperature of 20 K. The inset shows MDCs at  $E_F$  along several momentum cuts in one octant of the second Brillouin zone; the corresponding cuts are marked in the figure with a number from 1 to 9. The red cross in the figure represents the peak position of MDCs at  $E_F$ . (b1)–(b9) EDCs along the cuts as marked in (a). The red spectra are EDCs on the underlying Fermi surface. The green shades in (b1)–(b5) highlight the energy range (0–70 meV) within which sharp peaks are confined.

allows *all* low energy quasiparticles below 70 meV. Under the working of this mechanism, both low energy nodal and antinodal excitations become sharp Bogoliubov-Landau quasiparticles. The “Fermi surface” should also be taken in this context to reflect the fact that by that we mean the locus of the lowest energy quasiparticle excitations before the extra scattering on antinodal excitations is switched on. Then we ask what extra is needed to explain the antinodal spectral broadening.

One candidate that immediately comes to mind is the  $(\pi, \pi)$  magnetic fluctuation that produces “hot spots” on the Fermi surface, as previously proposed for Bi2212 [2]. We note that neutron scattering has revealed a significant difference in the magnetic response of LSCO and Bi2212. The  $(\pi, \pi)$  spin resonance mode observed in Bi2212 [15] is absent in LSCO. Instead, incommensurate magnetic peaks were observed at low energy (below 15 meV) [16–18] (inset of Fig. 3), which broaden rapidly with increasing energy although the magnetic fluctuation can persist up to 280 meV [19]. To check whether the low energy incommensurate magnetic fluctuation can be responsible for the lack of spectral peaks in the antinodal segments, first we shift the measured Fermi surface by the peak wave vectors of the magnetic excitation  $((\pi, \pi) \pm (2\delta, 0)$  and  $(\pi, \pi) \pm (0, 2\delta)$  with  $\delta$  being the incommensurability) to produce four Fermi surface replicas. Then we record the intersections of these replicas with the original Fermi surface. These intersections are hot spots where the quasiparticles will experience scattering from the incommensurate magnetic fluctuations. For  $x = 0.063$  and  $x = 0.09$  samples, the obtained hot spots do concentrate around the antinodes. However, for  $x = 0.15$  and  $x = 0.22$  samples, the above construction also leads to hot spots mainly near the antinodal segments but

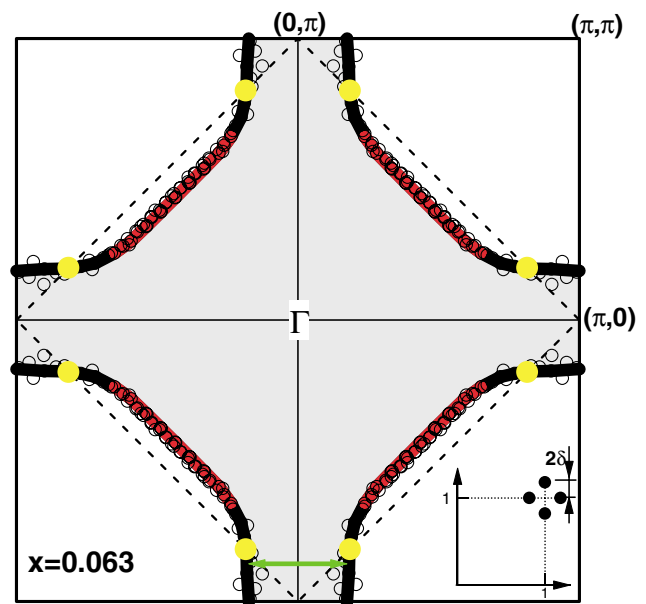


FIG. 3 (color). Experimental Fermi surface for LSCO  $x = 0.063$  sample. The black open circles are obtained from the MDC peak position at  $E_F$ , as shown in Fig. 1 as the red crosses, and then symmetrized in the first Brillouin zone. The solid lines are guides to the eye for the measured Fermi surface. The red lines represent the portion of Fermi surface where one can see quasiparticle peaks. The dotted black line represents the antiferromagnetic Brillouin zone boundary; its intersection with the Fermi surface gives eight “hot spots” (solid yellow circles) from  $(\pi, \pi)$  magnetic excitations. The double-arrowed green line represents a nesting vector,  $(0.35\pi, 0)$ , between the antinodal part of the Fermi surface. The inset shows the schematic neutron diffraction pattern observed in LSCO superconductors with four incommensurate peaks of distance  $2\delta$  from the  $(\pi, \pi)$  point.

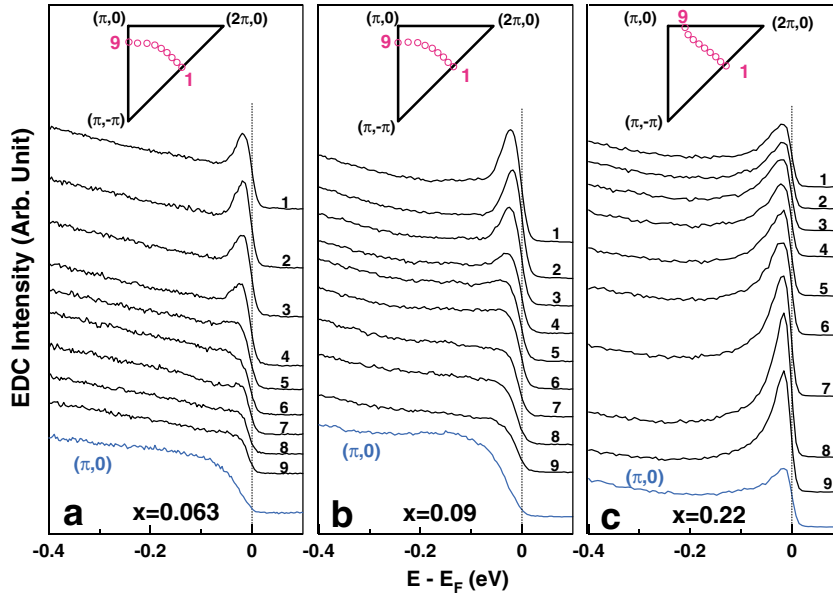


FIG. 4 (color). EDCs on Fermi surface for LSCO  $x = 0.063$  (a),  $0.09$  (b), and  $0.22$  (c) samples. All samples are measured at  $\sim 20$  K. The corresponding momentum position is marked in the upper inset of each panel. Also included are the spectra at  $(\pi, 0)$  points, colored as blue.

the quasiparticle peak can be seen over the entire Fermi surface. Considering that the incommensurate peaks are present in LSCO up to  $x = 0.25$  [18], this latter observation is inconsistent with the mechanism of the incommensurate magnetic fluctuations, although one cannot completely rule out this possibility because how the coupling strength varies with doping is not known.

Intrigued by the fact that the extra broadening sets in when the Fermi surface turns from the  $(\pi, 0)$ - $(0, \pi)$  diagonal direction to the  $(0, 0)$ - $(\pi, 0)$  or the  $(0, 0)$ - $(0, \pi)$  direction, we propose an alternative mechanism that the scattering in question causes a pair of electrons on two parallel antinodal segments to be scattered to the opposite ones (Fig. 3); i.e.,  $\mathbf{p}_1 = (\pm 0.175\pi, p_{1y})$ ,  $\mathbf{p}_2 = (\mp 0.175\pi, p_{2y}) \rightarrow \mathbf{p}'_1 = (\mp 0.175\pi, p_{1y})$ ,  $\mathbf{p}'_2 = (\pm 0.175\pi, p_{2y})$ , or  $\mathbf{p}_1 = (p_{1x}, \pm 0.175\pi)$ ,  $\mathbf{p}_2 = (p_{2x}, \mp 0.175\pi) \rightarrow \mathbf{p}'_1 = (p_{1x}, \mp 0.175\pi)$ ,  $\mathbf{p}'_2 = (p_{2x}, \pm 0.175\pi)$ . In the normal state, this scattering mechanism can cause a quasiparticle to decay into two quasiparticles and one quasihole. The antinodal spectral broadening occurs as a result of the frequent occurrence of such a decay which renders the normal state quasiparticle ill defined.

In summary, we have shown that the low energy excitations between nodal and antinodal quasiparticles behave very differently in the underdoped superconductors. Evidently such a dichotomy is due to the existence of an extra *low energy* scattering mechanism that operates primarily on antinodal quasiparticles. We propose this may be associated with quasiparticle scattering across the nearly parallel segments of the Fermi surface near the antinodes. Clearly, this proposal requires more scrutiny, both experimentally and theoretically.

The work at ALS and SSRL is supported by the DOE's Office of BES, Division of Material Science, under

Contract No. DE-FG03-01ER45929-A001. The work at Stanford was also supported by NSF Grant No. DMR-0304981 and ONR Grant No. N00014-98-1-0195-P0007. The work in Japan is supported by a Grant-in-Aid from the Ministry of Education, Culture, Sports, Science and Technology and NEDO. The work in China is supported by NSF of China and Ministry of Science and Technology of China through Projects No. 10174090 and No. G1999064601.

- [1] P.W. Anderson and R. Schrieffer, *Phys. Today* **44**, No. 6, 54 (1991).
- [2] Z.-X. Shen and J.R. Schrieffer, *Phys. Rev. Lett.* **78**, 1771 (1997).
- [3] D.L. Feng *et al.*, *Phys. Rev. Lett.* **86**, 5550 (2001); Y.D. Chuang *et al.*, *Phys. Rev. Lett.* **87**, 117002 (2001); P.V. Bogdanov *et al.*, *Phys. Rev. B* **64**, 180505(R) (2001).
- [4] T.K. Kim *et al.*, *Phys. Rev. Lett.* **91**, 167002 (2003).
- [5] M. Eschrig and M.R. Norman, *Phys. Rev. Lett.* **89**, 277005 (2002).
- [6] A.D. Gromko *et al.*, *Phys. Rev. B* **68**, 174520 (2003).
- [7] X.J. Zhou *et al.*, *Phys. Rev. Lett.* **86**, 5578 (2001).
- [8] T. Yoshida *et al.*, *Phys. Rev. B* **63**, 220501 (2001).
- [9] X.J. Zhou *et al.*, *Nature (London)* **423**, 398 (2003).
- [10] F. Zhou *et al.*, *Supercond. Sci. Technol.* **16**, L7 (2003).
- [11] P.V. Bogdanov *et al.*, *Phys. Rev. Lett.* **85**, 2581 (2000).
- [12] A. Kaminski *et al.*, *Phys. Rev. Lett.* **86**, 1070 (2001).
- [13] A. Lanzara *et al.*, *Nature (London)* **412**, 510 (2001).
- [14] P.D. Johnson *et al.*, *Phys. Rev. Lett.* **87**, 177007 (2001).
- [15] H.F. Fong *et al.*, *Nature (London)* **398**, 588 (1999).
- [16] J.M. Tranquada *et al.*, *Nature (London)* **375**, 561 (1995).
- [17] G. Aeppli *et al.*, *Science* **278**, 1432 (1997).
- [18] K. Yamada *et al.*, *Phys. Rev. B* **57**, 6165 (1998).
- [19] S.M. Hayden *et al.*, *Phys. Rev. Lett.* **76**, 1344 (1996).